

Synthesis, Optimization and Antibacterial Performance of Colloidal Silver Nanoparticles in Chitosan

Endang Susilowati*, Lina Mahardiani, Sri Retno Dwi Ariani, and Ilham Maulana Sulaeman

Department of Chemistry Education, Faculty of Teacher Training and Education, Universitas Sebelas Maret, Jl. Ir. Sutami 36A, Surakarta 57126, Indonesia

* **Corresponding author:**

email: endang_s70@staff.uns.ac.id

Received: May 26, 2023

Accepted: July 13, 2023

DOI: 10.22146/ijc.84822

Abstract: Colloidal silver nanoparticles were successfully synthesized via the chemical reduction method. The synthesis used AgNO_3 as the precursor, chitosan as the reducing and stabilizing agents, and NaOH as the accelerator. The synthesis parameters were optimized. The samples were tested with a UV-vis spectrophotometer to observe their localized surface plasmon resonance (LSPR) phenomenon, a transmission electron microscope (TEM), and a particle size analyzer (PSA) to investigate their particle shape and size distribution. Further, silver nanoparticles were tested for their storage stability and antibacterial performance. The UV-vis spectroscopy data exhibited that the silver nanoparticles have been successfully synthesized, validating via the emergence of the LSPR absorption band at 402–418 nm. At 50 °C, the optimum synthesis was achieved for 100 min of reaction time by adding 0.033 M NaOH and AgNO_3 4.00% (w/w, AgNO_3 /chitosan). TEM results showed spherical silver nanoparticles of 1–8 nm, while the PSA results exhibited particles sizes of about 12–59 nm. The colloidal silver nanoparticles were stable in storage for 8 weeks and had good antibacterial performance against *E. coli*, *S. aureus*, extended-spectrum beta-lactamases (ESBL), and methicillin-resistant *S. aureus* (MRSA). Therefore, colloidal silver nanoparticles have the potential as a material for medical applications.

Keywords: antibacterial performance; colloidal silver nanoparticles; chitosan; synthesis optimization

■ INTRODUCTION

The health sector is crucial in human life, so things related to medicine are constantly being developed. Studies regarding new antibacterial materials are fascinating because of the growing demand for medical applications. One of the developed materials for the fabrication of antibacterial agents is chitosan. Chitosan is a natural polymer derived from chitin isolated from fishery garbage, such as shrimp and crab shells. Chitin is a natural biopolymer found abundant after cellulose [1]. The result of the deacetylation of chitin is called chitosan, which has many benefits because of its properties, namely non-toxic compound possessing excellent biodegradability, antibacterial and antifungal characteristics, and biocompatibility [2].

Chitosan has antibacterial performance as a result of the existence of positively charged clusters $[-\text{NH}_3^+]$ which will interact with the negative charges on the bacterial cell membrane and change the cell permeability properties [2]. However, the antibacterial performance of chitosan is still relatively low and depends on the pH [3]. The pH has been considered as the most significant factor that influences the antimicrobial activity of chitosan. It impacts the solubility and the electrical charge of chitosan molecules. So, this is a limitation of chitosan as an antibacterial. The antibacterial performance of chitosan can be advanced by adding other antibacterial materials. Silver nanoparticles include metal nanoparticles often studied and act as antibacterial material [4]. Completed with their antimicrobials [5], anti-inflammatory [6], and drug

delivery systems [7], silver nanoparticles are commonly applied to the medical world. The incorporation of silver nanoparticles into chitosan can produce a colloidal silver nanoparticle system.

Silver nanoparticles can be synthesized with numerous methods. Still, chemical reduction is the most commonly employed method because it is easy, simple, and effective that could yield satisfactory results [8]. Besides, the method is relatively affordable and can be performed on large-scale production. In general, metal nanoparticle synthesis with this method requires a reductant to reduce metal ions and a stabilizer to stabilize the nanoparticles [9]. Reducing agents widely used are sodium borohydride, sodium citrate, ascorbate, and Tollens reagent. One of these is sodium borohydride (NaBH_4), which is the most commonly used reducing agent in synthesizing silver nanoparticles. This is because NaBH_4 is a potent reducing agent that can reduce the temperature and reduction time of silver metal ions. However, the usage of this chemical in the synthesis can lead to health and environmental problems [10].

Considering this matter, it is necessary to develop a green synthesis to produce silver nanoparticles. Several scientists have established the usage of environmentally friendly weak reducing agents such as liginosulphonate acid [10], banana peel extract [11], *n*-hexane extract of *Malachra capitata* (L.) leaf [12], glucose [13], and chitosan [14]. Chitosan is a biopolymer that can reduce metal ions, enabling the synthesis of nanoparticles of controlled shape, size, and stability [14].

Chitosan is an attractive reducing agent to be studied because it can act as a stabilizer simultaneously. Referring to previous research, chitosan could reduce silver ions, but it required a high temperature (95 °C) and a relatively long reaction time (12 h) [15]. Meanwhile, other studies succeeded in synthesizing silver nanoparticles with glucose as a reducing agent, gelatin as a stabilizer, and NaOH as an accelerator which only required 60 °C temperature and 15 min reaction time [16]. Reducing silver ions with a weak reducing agent such as glucose is effective when conducted under alkaline conditions [13]. This study provides a solution to synthesize silver nanoparticles using chitosan as a

reducing agent and NaOH as an accelerator to reduce the temperature and the formation time of silver nanoparticles. Synthesis optimization of silver nanoparticles in chitosan needs to be done to find the synthesis conditions with the best and most efficient results. Furthermore, this result will be important to be applied for producing antibacterial materials for medical applications, especially for wound dressing.

Various stabilizing agents, such as gelatin [16] and polyvinyl alcohol [17] at different concentrations, affect the size and shape of the resulting silver nanoparticles. Chitosan is one of the stabilizing agents to be examined because of its ability as a stabilizer and antibacterial properties. Studies on silver nanoparticle synthesis using chitosan as the stabilizing agent have been conducted previously [18-19]. Stabilizing agents are essential to control the formation of well-dispersed nanoparticles with uniform particle sizes. Silver nanoparticles yield a colloidal system when dispersed in a chitosan solution.

Here, colloidal silver nanoparticles were synthesized with AgNO_3 as the precursor, chitosan as the reducing and stabilizing agent, and NaOH as the accelerator. The synthesis parameters were optimized to determine the best conditions by varying reaction temperature and time, NaOH concentration, and AgNO_3 concentration. Besides, the antibacterial performance of colloidal silver nanoparticles was tested against standard bacteria (*E. coli* and *S. aureus*) and multiresistant bacteria (ESBL and MRSA).

■ EXPERIMENTAL SECTION

Materials

The starting materials were chitosan made from crab shells (Biotech Surindo Indonesia), glacial acetic acid (CH_3COOH), silver nitrate (AgNO_3), and sodium hydroxide (NaOH) (Merck); and distilled water from Integrated Laboratory of Universitas Sebelas Maret, Indonesia.

Instrumentation

To characterize the formation of silver nanoparticles, the UV-vis Shimadzu UV-1800 spectrophotometer was used. The shape and size

distribution of the particles were characterized using the JIOL JEM-1400 series transmission electron microscope (TEM) instrument with a voltage of 80 KeV. The particle size distribution was also tested using the Malvern Zetasizer particle size analyzer (PSA).

Procedure

First, chitosan was diluted in 0.5% (v/v) CH₃COOH solution, producing a 0.5% (w/v) chitosan solution. Then, 12.5 mL of 0.5% chitosan solution was added into 0.8 mL of AgNO₃ solution (0.01 g/mL) while stirred for 5 min. Next, it was added with 1.25 mL of NaOH (2 M) solution while stirring for 5 min, forming a gel in the solution with the color changing to brown. The solution was then treated with temperature variations at room temperature (26 °C), 30, 40, 50, and 60 °C for 90 min. Afterward, 47.5 mL of 0.5% chitosan was added to each solution and stirred until completely dissolved. The resulting colloid was put into bottles and stored at room temperature.

The same process was performed to optimize the synthesis of silver nanoparticles with the independent and dependent variables, as shown in Table 1. The silver nanoparticle samples with various concentrations of AgNO₃ were then tested for stability in storage for 8 weeks based on the LSPR phenomenon characterized via a UV-vis spectrophotometer.

This procedure of analysis was completed to ensure the successful synthesis of the silver nanoparticles through the LSPR phenomenon. The first step was diluting the samples into distilled water as much as 10

times. The solution was then tested with a UV-vis Shimadzu UV-1800 spectrophotometer to measure the absorbance and maximum wavelength in the wavelength range (λ) of 600–300 nm.

Analysis using TEM and PSA was performed to examine the particle shape and size distribution. In this step, the samples were thinned and then placed in a copper grid. Then, the samples were observed using the TEM instrument with a voltage of 80 KeV. The particle shape and size distribution were determined manually. The samples were also analyzed with the Malvern Zetasizer PSA to investigate the particle size distribution. Before testing, the colloid samples were diluted and filtered.

The antibacterial performance of colloidal silver nanoparticles with various AgNO₃ concentrations was tested against *S. aureus* ATCC 25922, *E. coli* ATCC 25923, MRSA, and ESBL with the well-diffusion method in duplicate [20]. Tests were carried out using Mueller Hinton Agar (MHA) as a material medium. The MHA solid media smeared with bacteria was perforated with a diameter of 7 mm and then filled with 50 μL of colloidal silver nanoparticles samples. It was then followed by incubation at 37 °C for 24 h. The clear zone which is the diameter of the inhibition zone is measured using a digital caliper.

RESULTS AND DISCUSSION

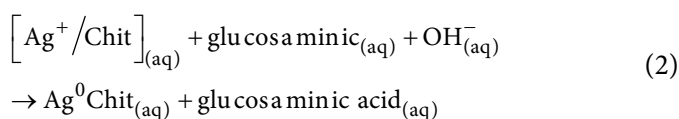
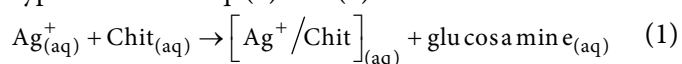
Here, colloidal silver nanoparticles have been successfully synthesized by the chemical reduction

Table 1. Synthesis condition for the optimization process

No	Independent variables	Dependent variables
1	Temperature = 26, 30, 40, 50, and 60 °C	Time = 90 min [NaOH] = 0.042 M [AgNO ₃] = 2.66%
2	Time = 20, 40, 60, 80, 100, and 120 min	Temperature = 50 °C [NaOH] = 0.042 M [AgNO ₃] = 2.66%
3	[NaOH] = 0, 0.008, 0.017, 0.025, 0.033, 0.042, 0.050, 0.058, and 0.067 M	Temperature = 50 °C Time = 100 min [AgNO ₃] = 2.66%
4	[AgNO ₃] = 0.66, 1.33, 2.00, 2.66, 3.33 and 4.00%	Temperature = 50 °C Time = 100 min [NaOH] = 0.033 M

procedure. This research applied green synthesis because the chemicals used are non-toxic, environmentally friendly solvents and renewable materials. The synthesis employed AgNO_3 as the silver precursor, chitosan as the reducing and stabilizing agents, and NaOH as the accelerator. The prior study performed chitosan as the reducing agent to synthesize gold nanoparticles under alkaline environments through hydrolysis and degradation to yield glucosamine [21]. Thus, associated with this study, glucosamine will reduce metal ions to yield silver zero valences and glucosaminic acid. It is similar to reducing glucose under alkaline conditions [13-16].

In this study, the colloid color changed from transparent to yellow to brown, denoting the success of the silver nanoparticle formation [16]. This color appeared as a result of the LSPR phenomenon. Metallic surfaces possess free electrons in the conduction band (CB) and a positively charged nucleus [8]. LSPR is the electron excitation group in the CB nearby the surface of the nanoparticles. Metal nanoparticles exhibit a particular absorption spectrum on the surface so that the LSPR phenomenon can be detected by UV-vis spectrophotometer [18]. The LSPR band of silver nanoparticles produces a typical absorption band spectrum in the 400–450 nm wavelength range [22]. Here, the mechanism for the silver nanoparticles formation is hypothesized as Eq. (1) and (2).



When AgNO_3 is added to the chitosan solution, Ag^+ ions will be chelated in the chitosan structure by forming coordinate bonds with amino groups ($-\text{NH}_2$) and hydroxyl ($-\text{OH}$) written as $[\text{Ag}^+/\text{Chit}]$. In the next step, by adding the NaOH accelerator containing OH^- ions, the glucosamine group from chitosan can perform as a reducing agent, which converts Ag^+ ions into metal Ag and glucosaminic acid as a result of the oxidation of glucosamine. Ag crystal growth will be limited by chitosan polymer so that Ag with nano size (< 100 nm) can be obtained.

Synthesis Optimization of Silver Nanoparticles

The effects of heating temperatures on the LSPR band were observed. The temperature variations were 26, 30, 40, 50, and 60 °C with 90 min reaction time, 0.042 M NaOH , and AgNO_3 2.66% (w/w; $\text{AgNO}_3/\text{chitosan}$). Fig. 1(a) shows that the resulting colloid is darker with higher heating temperatures. Temperature is an important aspect significantly affecting the synthesis results of colloidal silver nanoparticles. The typical LSPR band for silver nanoparticles is about 407–418 nm. The heating temperature is directly proportional to the absorbance produced. The higher temperature leads to greater absorbance, denoting an enhancement in the concentration of silver nanoparticles [5]. The absorbance band due to LSPR silver nanoparticles experience a blue shift from 418 to 407 nm as the increasing temperature from 30 to 60 °C, revealing that the sizes of silver nanoparticles decrease with the higher heating temperature. It is considered because of the rapid reaction rate at high temperatures. At high temperatures, the kinetic energy is enhanced, so silver ions are reduced more rapidly, thereby reducing the possibility of particle size growth. Consequently, at higher heating temperatures, smaller particles with uniform distribution are produced [5]. In this variation, the temperature of 50 °C was chosen for optimization of other parameters because it had a high absorbance, which was slightly different from the temperature of 60 °C and was more efficient from the aspect of energy use.

Furthermore, the influence of reaction time on the LSPR band was also investigated. Fig. 1(b) presents the UV-vis absorption spectra and colloid color for each sample. In general, the absorbance improves with increasing heating time. It shows that the longer heating time causes a greater amount of silver nanoparticles to be produced. However, the samples have almost the same absorbance values at 100 and 120 min. It means that, at a certain time, the silver nanoparticles produced will be constant, where the formation of silver nanoparticles will no longer occur because the silver nitrate has been completely reduced [5]. The typical LSPR band for silver nanoparticles was about 410–414 nm.

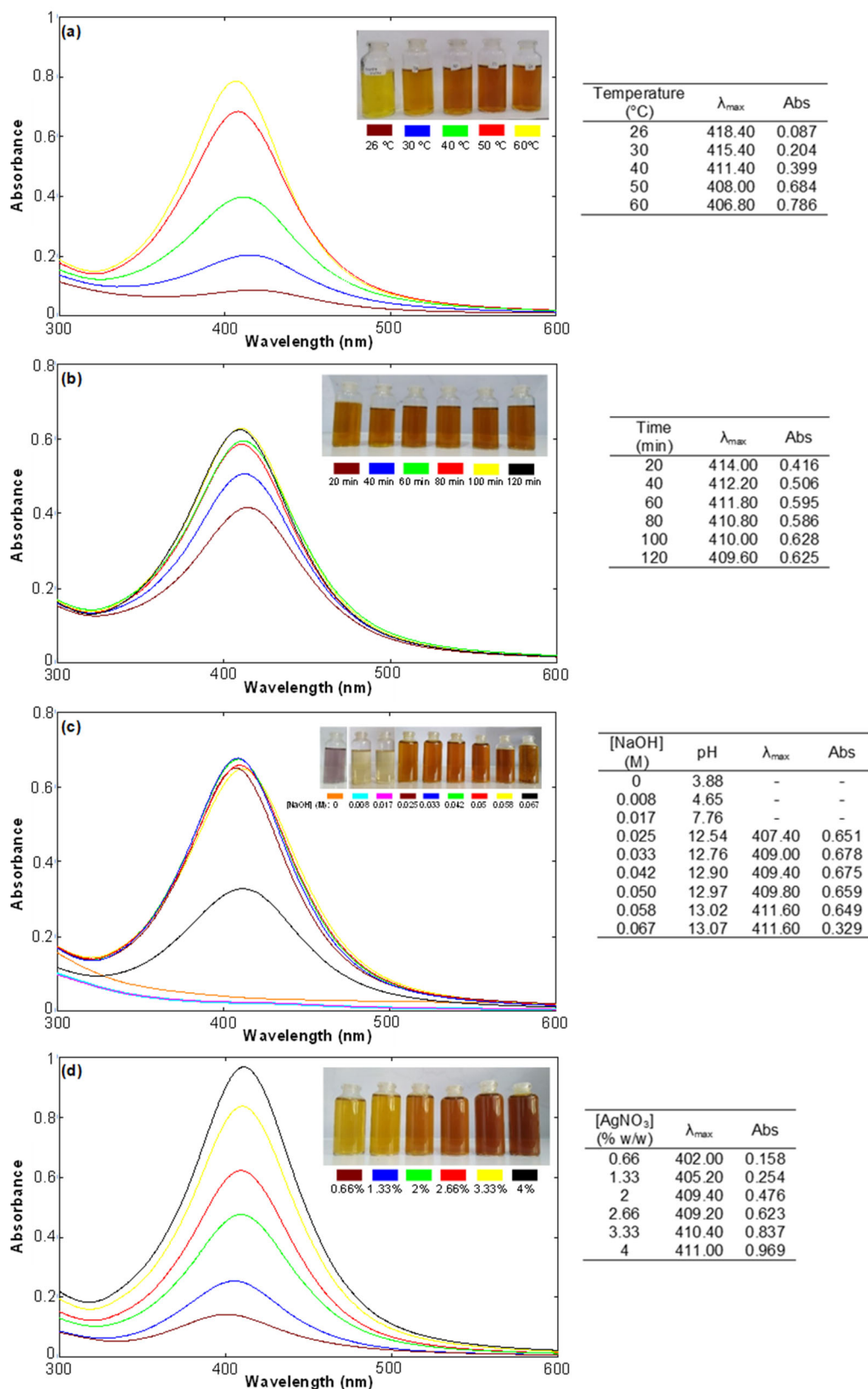


Fig 1. UV-vis spectrum of colloidal silver nanoparticles with variations: (a) temperature, (b) reaction time, (c) NaOH concentration, and (d) AgNO₃ concentrations

The absorbance band due to LSPR silver nanoparticles experience a blue shift (20–120 min), exhibiting that the sizes of the silver nanoparticles decline with the longer heating time. The optimal reaction time needed for forming silver nanoparticles was 100 min since, after that, no addition of silver nanoparticles was observed.

In this study, NaOH acts as an accelerator, added to provide time efficiency and effectiveness in preparing silver nanoparticles. Fig. 1(c) shows that the resulting colloid's color tended to be darker with a higher NaOH concentration. However, at NaOH concentrations of 0.025–0.067 M, the colloid did not exhibit a significant color gradation. It implies that the silver nitrate in the colloid has been completely reduced [5]. In comparison, at the concentration of 0, 0.008, and 0.017 M, the colloid did not experience a color change to brown, which might be because the colloid does not contain silver nanoparticles. Based on Fig. 1(c), the LSPR band could not be identified without NaOH addition. Besides, it also could not be identified with the addition of a small amount of NaOH at the concentrations of 0.008 and 0.017 M. The absorbance values at the NaOH concentration of 0.025–0.058 M differed slightly. The absorbance enhanced from 0.025 to 0.033 M concentrations, indicating that the higher NaOH concentration resulted in a more significant number of silver nanoparticles. However, the introduction of NaOH further declined the absorbance (concentrations of 0.042–0.067 M) and significantly decreased at 0.067 M.

It is considered due to the construction of a denser gel at a higher NaOH concentration which inhibits the reduction of silver ions to silver nanoparticles [13]. At the NaOH concentrations of 0, 0.008, and 0.017 M, the colloidal silver nanoparticles had a pH value of less than 8 and did not exhibit an absorbance band. In contrast, at concentrations of 0.025–0.067 M, they had a pH value above 12, which emerged absorbance band. These follow the results of previous research, where a pH of about 9–13 is the most ideal for synthesizing silver nanoparticles [5]. The typical LSPR band for silver nanoparticles was at 407–412 nm wavelength. The absorbance band due to LSPR silver nanoparticles experienced a red shift at the NaOH concentrations of 0.042–0.067 M, demonstrating

an enlargement in the size of silver nanoparticles as the higher NaOH concentration. The optimal NaOH concentration needed to form silver nanoparticles was 0.033 M since, after that, no addition of the silver nanoparticles number was observed.

Next, the influence of AgNO₃ concentration on the LSPR band was observed. Fig. 1(d) shows that the higher AgNO₃ concentration led to a darker color of the colloid produced. The higher AgNO₃ concentration from samples 0.66–4.00% was proportional to the increase in the absorbance value. The typical LSPR band for silver nanoparticles is at 402–411 nm wavelength. The emergence of the LSPR absorption band at around 400 nm demonstrates that the particles are spherical [8]. The absorbance band due to LSPR silver nanoparticles experienced a redshift (0.66–4.00%), revealing that the sizes of silver nanoparticles enlarge as the higher AgNO₃ concentration. Colloidal silver nanoparticles with a further variation of AgNO₃ concentration were then tested for their stability and antibacterial performance.

Based on the results of the optimization parameters of temperature (Fig. 1(a)), time (Fig. 1(b)), and NaOH concentration (Fig. 1(c)), the optimal conditions for synthesizing silver nanoparticles were at 50 °C for 100 min with 0.033 M NaOH. These results are more efficient than similar research reported by Kalaivani et al. [23], where silver nanoparticles were synthesized at 90 °C for 10 h.

The higher AgNO₃ concentration induced a higher absorbance, indicating a higher concentration of silver nanoparticles formed. Fig. 2 shows that the relationship between the AgNO₃ concentration was linearly proportional to the absorbance with a coefficient of determination of $R^2 = 0.992$. It strengthens the argument that the higher AgNO₃ concentration used induces, the greater concentration of silver nanoparticles yielded.

Stability of Colloidal Silver Nanoparticles

Colloidal silver nanoparticles are called stable if the concentration, size, and shape of the particles do not change. The concentration of silver nanoparticles correlates with the absorbance intensity in the UV-vis spectra. Therefore, the stability of silver nanoparticles can

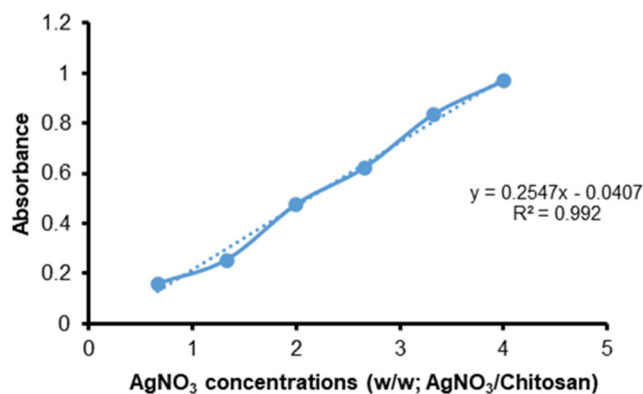


Fig 2. Relationship between concentration precursor of AgNO₃ and absorbance

be investigated based on their absorbance and maximum wavelength. The stability of colloidal silver nanoparticles was carried out by measuring the absorbance and maximum wavelength at various AgNO₃ concentrations every week for 8 weeks. Colloidal silver nanoparticles were stored at room temperature. Before measurement, the samples were diluted 10 times into distilled water. The change in the LSPR band of the UV-vis spectrum is presented in Fig. 3(a) and 3(b). Absorbance for AgNO₃ concentration of 0.66–4% (w/w; AgNO₃/chitosan) tended to decrease at week 1 of storage compared to weeks 2–8. This indicates that, in the first week, there may be more silver nanoparticle aggregation than in weeks 2–8. At lower concentrations, silver nanoparticles tended to be more stable than at high concentrations (Fig. 3(a)).

The results of the UV-vis absorption spectra also showed maximum wavelength data for each sample. The samples experienced a shift in the maximum wavelength to the right and the left, but only slightly. Seen from the

maximum wavelength, it tended to be a red shift in all samples, indicating a larger particle size during storage (Fig. 3(b)). This is in line with the decreasing absorption band, demonstrating that silver nanoparticles tend to experience aggregation during storage. These results differ from previous studies, where silver nanoparticles were still stable after week 8 of storage using glucose as a reducing agent and chitosan as a stabilizer [13].

TEM Analysis

TEM analysis was employed to observe the shape and size distribution of silver nanoparticles in the colloidal system. The samples observed were AgNO₃ with concentrations of 2.66 and 4.00% (w/w; AgNO₃/chitosan), respectively. These two samples represented the observed particle size distribution of silver at low and high concentrations using TEM. The emergence of the LSPR absorption band at about 400 nm denotes the spherical-shaped particles that follow the resulting TEM images in the previous report [8]. Based on Fig. 4(a) and 4(b), the use of AgNO₃ as silver nanoparticle precursor with a concentration of 4.00% produced more silver nanoparticles than AgNO₃ at 2.66%. The TEM image of Sample A4 exhibits flakes on the sample. It may be due to the colloid preparation that is too thick.

The higher AgNO₃ concentration induces a higher concentration of silver nanoparticles [14]. In the same area, there were 65 particles at the AgNO₃ concentration of 2.66% and 95 particles at the AgNO₃ of 4.00%, calculated with the ImageJ application. It is in line with the rise in absorbance from 0.623 to 0.969 (Fig. 1(d)). Fig. 5(a) and 5(b) show that, at the AgNO₃ concentration

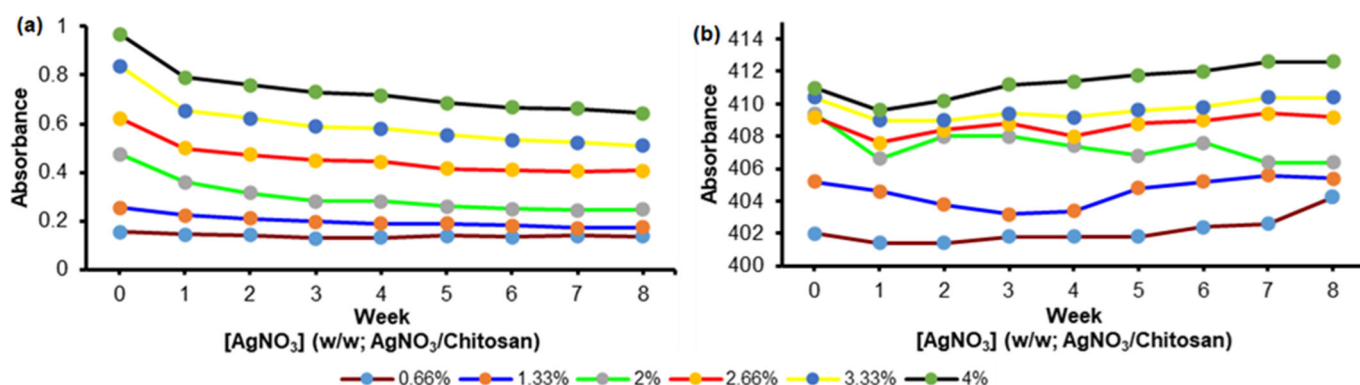


Fig 3. Stability of colloidal silver nanoparticles changes in (a) absorbance and (b) maximum wavelength

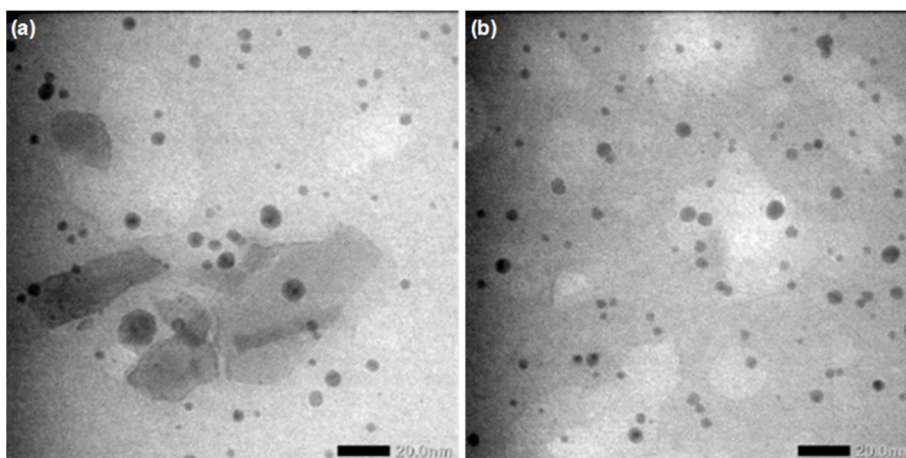


Fig 4. TEM images of colloidal silver nanoparticles (a) 2.66% and (b) 4.00% (w/w; AgNO₃/chitosan)

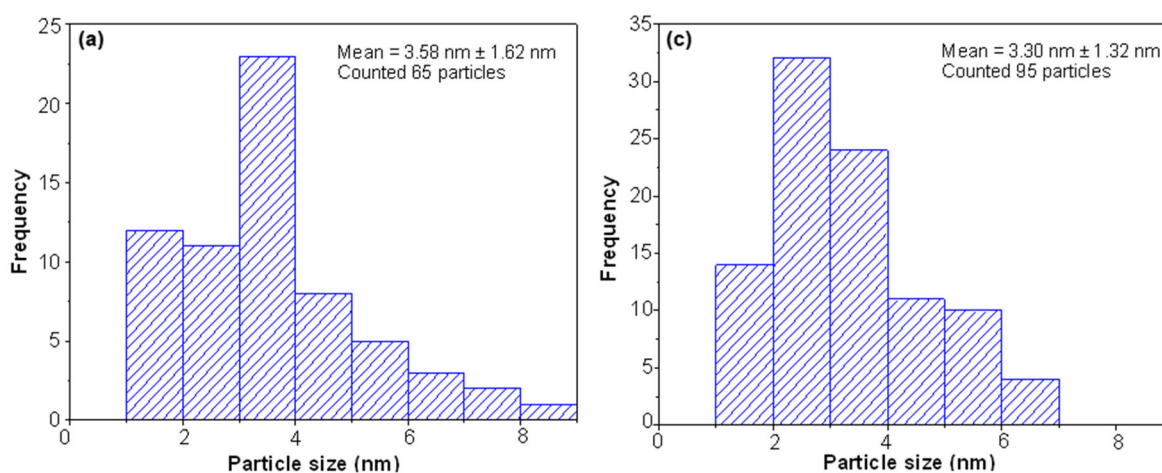


Fig 5. Size distribution of colloidal silver nanoparticles (a) 2.66% and (b) 4.00% (w/w; AgNO₃/chitosan)

of 2.66%, the average particle diameter was 3.58 nm with a range of 1–8 nm. In contrast, at the AgNO₃ concentration of 4.0, the average particle diameter was 3.30 nm, with a 1–7 nm range. Thus, the particle size at the AgNO₃ concentration of 2.66% was slightly larger than at 4.00%. It does not align with the LSPR absorption band, which reveals a redshift from 409.20 to 411.00 nm. In this study, the slight difference in maximum wavelength does not significantly affect the particle size. According to the distribution frequency, silver nanoparticles were conquered by particles with 2–4 nm size. On the other, the results of other researchers who have synthesized silver nanoparticles using *Malachra capitata* (L.) leaf showed that the particle size ranged from 30 to 35 nm with an average diameter of 35 nm. The size distribution curve revealed that the particles ranged from 5–70 nm, and the mean particle

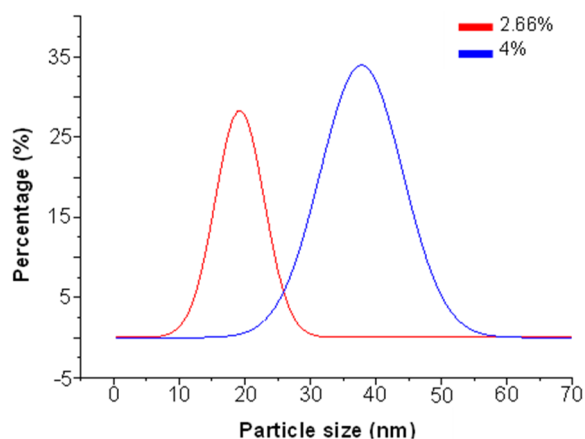
diameter was about 5 nm [12]. It shows that previous research obtained a larger particle size than this research.

PSA Analysis

PSA was completed to observe the size and distribution of silver nanoparticles. The samples analyzed were AgNO₃ with 2.66 and 4.00% concentrations (w/w; AgNO₃/chitosan), respectively. Here, the distribution number was exploited to estimate the relative number of distribution percentages of each size (Fig. 6). Table 2 shows data on the polydispersity index (PDI), mean size, and standard deviation of samples with AgNO₃ concentrations of 2.66 and 4.00%. The particle sizes resulting from TEM were smaller than those from PSA. The particle sizes from TEM were 1–8 nm, while those from PSA were 12–38 nm (2.66%) and

Table 2. PSA characterization result

AgNO ₃ (as precursor)	PDI	Average size (nm)	Standard deviation (nm)
2.66%	0.341	19.80	4.569
4%	0.482	38.22	6.776

**Fig 6.** Particle size distribution of silver nanoparticles by frequency (%)

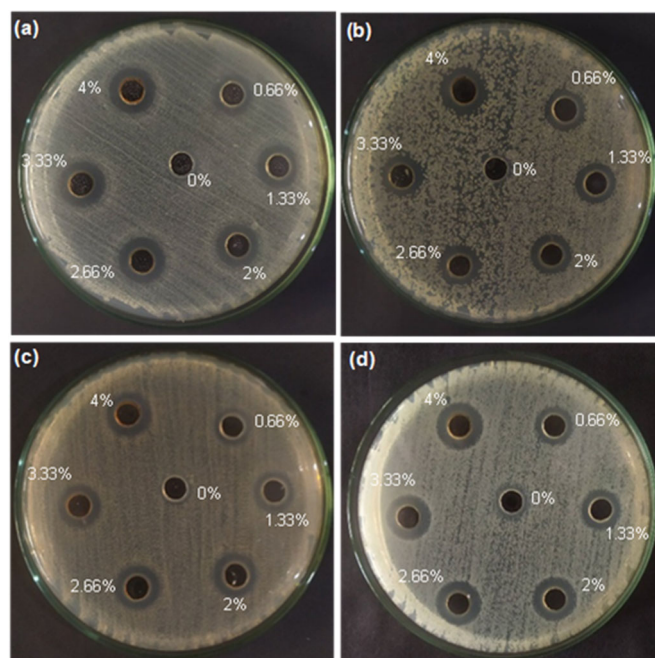
28–59 nm (4.00%). Measurement with PSA used a water dispersion medium so that the chance of small particles sticking together is enormous during the measurement. Thus, the particle size obtained is larger due to agglomeration. In addition, the particle size of the PSA characterization is a hydrodynamic diameter measure, where the particle size includes the Ag particles and the stabilizer agent surrounding the particles [24].

The polydispersity index (PDI) reveals the level of confidence in the size of the dispersed particles in colloidal silver nanoparticles. The PDI value closer to zero indicates a uniform particle. If the PDI value is greater than 0.7, it reveals high heterogeneity and is probably unsuitable for analysis by the dynamic light scattering (DLS) method [25]. The use of AgNO₃ with concentrations of 2.66 and 4.00% as a precursor for silver nanoparticles had a PDI value of less than 0.5, indicating a relatively good level of particle uniformity. The PDI value is associated with the standard deviation value and the particle size distribution curve presented in Fig. 6. The smaller PDI value means a lower standard deviation, representing high accuracy. At the AgNO₃ concentration of 2.66%, the standard deviation value was 4.569 nm, lower than that of a 4.00% concentration with a value of 6.776 nm. In addition, the

smaller PDI value means a narrower particle size distribution. The AgNO₃ concentration of 2.66% exhibited a narrower distribution curve than 4.00%, where the particle sizes were about 12–38 nm (2.66%) and 28–59 nm (4.00%). These results denote that the concentration of AgNO₃ as the silver nanoparticles precursor has an effect on particle size. At a high AgNO₃ concentration, a larger size of silver is produced.

Antibacterial Performance of Colloidal Silver Nanoparticles

The antibacterial performance of colloidal silver nanoparticles with diverse concentrations of AgNO₃ precursors represents the number of silver nanoparticles in colloids. The colloids tested were all samples with concentrations of 0.66–4.00% (w/w; AgNO₃/chitosan) and a chitosan solution without AgNO₃ for comparison. The ability of colloidal silver nanoparticles to inhibit the growth of bacteria was tested by the well-diffusion method. The bacteria included gram-positive bacteria (*S. aureus* and MRSA) and gram-negative bacteria (*E. coli* and ESBL). The results are presented in Fig. 7.

**Fig 7.** Inhibition area of colloidal silver nanoparticles with various AgNO₃ concentrations (w/w; AgNO₃/chitosan) against (a) *S. aureus*, (b) *E. coli*, (c) MRSA, and (d) ESBL

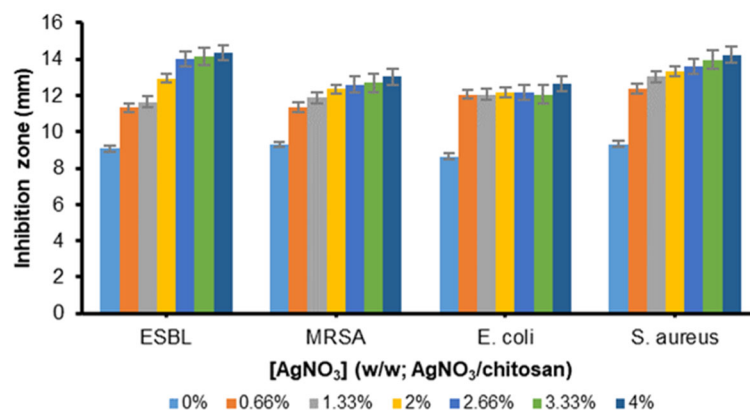


Fig 8. Antibacterial performance of colloidal silver nanoparticles

The antibacterial performance was examined based on the diameter of the inhibition area indicated by the appearance of a clear area around the hole comprising colloidal silver nanoparticles. The wide clear area suggests that the samples have high antibacterial performance and *vice versa*.

Two sources inhibiting bacterial growth are chitosan and silver nanoparticles. Chitosan solution (0% AgNO₃) had lower antibacterial performance than all colloidal silver nanoparticles with AgNO₃ concentrations of 0.66–4.00% as precursor silver nanoparticles. Previous researchers proposed several mechanisms for the inhibition of bacterial growth by chitosan; however, one mechanism is most believed. The mechanism is an interaction between the positive charges of chitosan (NH₃⁺) with the negative charges of the outer membrane of the microbial cell. It changes the structure and permeability of the cell membrane, contaminating proteins and other intracellular components. It thereby challenges the biochemical and physiological competence of the bacteria, causing the loss of replicative ability, and, eventually, the bacteria die [2].

Several factors influencing the antibacterial performance of silver nanoparticles are particle size, surface area, morphology, and distribution degree [26]. There are three most common mechanisms for silver nanoparticles in inhibiting bacterial growth: (1) Ag⁺ ions absorption followed by the interference of ATP construction and DNA replication, (2) silver nanoparticles and Ag⁺ ions making reactive oxygen species (ROS), and (3) silver nanoparticles directly devastating cell membranes [27].

Colloidal silver nanoparticles are a sol-colloid type system, so all three mechanisms can occur. When silver penetrates bacterial cells, some particles can release silver ions and silver nanoparticles at the same time, form ROS and then prevent ATP production and DNA replication. When the colloid diffuses in the bacterial medium, the silver nanoparticles insert the bacterial cell and impact the permeability and function of the membrane [18].

Chitosan solution without silver nanoparticles possessed the smallest diameter of the inhibition area compared to others (0.66–4.00% AgNO₃ concentrations). Thus, it is proven that the addition of silver nanoparticles could increase antibacterial performance. Colloidal silver nanoparticles had good antibacterial performance against all bacteria tested, both non-multiresistant bacteria (*S. aureus* and *E. coli*) and multiresistant bacteria (MRSA and ESBL). Based on Fig. 8, in general, the increase in AgNO₃ concentration was in line with the enlargement in the diameter of the inhibition area in the four bacteria. This means that colloidal silver nanoparticles with higher concentrations have higher antibacterial activity.

CONCLUSION

Colloidal silver nanoparticles were successfully formed by chemical reduction. Chitosan acted as the reducing and stabilizing agents, and NaOH was the accelerator. The silver nanoparticles formed were confirmed with the emergence of the LSPR absorption band at 402.0–418.4 nm. At 50 °C and 4.00% (w/w)

AgNO₃ concentration, the synthesis of colloidal silver nanoparticles was optimal at 100 min of reaction time with a concentration of 0.033 M NaOH. Based on the LSPR phenomenon identified by the UV-vis spectrophotometer, colloidal silver nanoparticles were stable in storage for 8 weeks at room temperature. The nanoparticles were spherical with 1–8 nm size based on the TEM analysis, while from the PSA analysis, the particle size was 12–59 nm. The higher silver nanoparticle concentration in colloidal resulted in higher antibacterial performance against *S. aureus*, *E. coli*, MRSA, and ESBL.

■ ACKNOWLEDGMENTS

The acknowledgment is delivered for the Directorate of Research, Technology and Community Service, Directorate General of Higher Education, Research and Technology of Indonesia, which funded this research through the *Penelitian Unggulan Perguruan Tinggi* (PDUPT) grant 2022 in Universitas Sebelas Maret with contract number 1035.1/UN27.22/PT.01.03/2022.

■ AUTHOR CONTRIBUTIONS

Endang Susilowati conducted the conceptualization, project leader, project administration, supervision, writing the original and revision of the manuscript. Lina Mahardiani contributed on translation, editing, and revision of the manuscript. Sri Retno Dwi Ariani was responsible for analysis data and editing the original manuscript. Ilham Maulana Sulaeman conducted the experiments and analysis data.

■ REFERENCES

- [1] Iber, B.T., Kasan, A., Torsabo, D., and Omuwa, J.W., 2022, A review of various sources of chitin and chitosan in nature, *J. Renewable Mater.*, 10 (4), 1097–1123.
- [2] Badawy, M.E.I., and Rabea, E.I.A., 2011, A biopolymer chitosan and its derivatives as promising antimicrobial agents against plant pathogens and their applications in crop protection, *Int. J. Carbohydr. Chem.*, 2011, 460381.
- [3] Ardean, C., Davidescu, C.M., Nemeş, N.S., Negrea, A., Ciopec, M., Duteanu, N., Negrea, P., Duda-Seiman, D., and Musta, V., 2021, Factors influencing the antibacterial activity of chitosan and chitosan modified by functionalization, *Int. J. Mol. Sci.*, 22 (14), 7449.
- [4] Valverde-Alva, M.A., García-Fernández, T., Villagrán-Muniz, M., Sánchez-Aké, C., Castañeda-Guzmán, R., Esparza-Alegria, E., Sánchez-Valdés, C.F., Llamazares, J.L.S., and Herrera, C.E.M., 2015, Synthesis of silver nanoparticles by laser ablation in ethanol: A pulsed photoacoustic study, *Appl. Surf. Sci.*, 355, 341–349.
- [5] Verma, A., and Mehata, M.S., 2015, Controllable synthesis of silver nanoparticles using neem leaves and their antimicrobial activity, *J. Radiat. Res. Appl. Sci.*, 9 (1), 109–115.
- [6] David, L., Moldovan, B., Vulcu, A., Olenic, L., Perde-Schrepler, M., Fischer-Fodor, E., Florea, A., Crisan, M., Chiorean, I., Clichici, S., and Filip, G.A., 2014, Green synthesis, characterization and anti-inflammatory activity of silver nanoparticles using European black elderberry fruits extract, *Colloids Surf., B*, 122, 767–777.
- [7] Gholamali, I., Asnaashariisfahani, M., and Alipour, E., 2020, Silver nanoparticles incorporated in pH-sensitive nanocomposite hydrogels based on carboxymethyl chitosan-poly (vinyl alcohol) for use in a drug silver system, *Regener. Eng. Transl. Med.*, 6 (2), 138–153.
- [8] Guzmán, M.G., Dille, J., and Godet, S., 2009, Synthesis of silver nanoparticles by chemical reduction method and their antibacterial activity, *Int. J. Chem. Biomol. Eng.*, 2 (3), 104–111.
- [9] Iravani, S., Korbekandi, H., Mirmohammadi, S.V., and Zolfaghari, B., 2014, Synthesis of silver nanoparticles: Chemical, physical and biological methods, *Res. Pharm. Sci.*, 9 (6), 385–406.
- [10] Reddy, G., and Thakur, A., 2017, Biogenic synthesis of silver nanoparticles using plant waste material, *Rasayan J. Chem.*, 10 (3), 695–699.
- [11] Ibrahim, H.M.M., 2015, Green synthesis and characterization of silver nanoparticles using banana peel extract and their antimicrobial activity against representative microorganisms, *J. Radiat. Res. Appl. Sci.*, 8 (3), 265–275.

- [12] Srirangam, G.M., and Rao, K.P., 2017, Synthesis and characterization of silver nanoparticles from the leaf extract of *Malachra capitata* (L.), *Rasayan J. Chem.*, 10 (1), 46–53.
- [13] Susilowati, E., Triyono, T., Santosa, S.J., and Kartini, I., 2015, Synthesis of silver-chitosan nanocomposites colloidal by glucose as reducing agent, *Indones. J. Chem.*, 15 (1), 29–35.
- [14] Susilowati, E., Masykuri, M., Ulfa, M., and Puspitasari, D., 2020, Preparation of silver-chitosan nanocomposites colloidal and film as antibacterial material, *JKPK*, 5 (3), 300–310.
- [15] Wei, D., Sun, W., Qian, W., Ye, Y., and Ma, X., 2009, The synthesis of chitosan-based silver nanoparticles and their antibacterial activity, *Carbohydr. Res.*, 344 (17), 2375–2382.
- [16] Darroudi, M., Ahmad, M., Abdullah, A.H., and Ibrahim, N.A., and Shameli, K., 2010, Effect of accelerator in green synthesis of silver nanoparticles, *Int. J. Mol. Sci.*, 11 (10), 3898–3905.
- [17] Ardani, H.K., Imawan, C., Handayani, W., Djuhana, D., Harmoko, A., and Fauzia, V., 2017, Enhancement of the stability of silver nanoparticles synthesized using aqueous extract of *Diospyros discolor* Willd. leaves using polyvinyl alcohol, *IOP Conf. Ser.: Mater. Sci. Eng.*, 188, 012056.
- [18] Susilowati, E., Maryani, M., and Ashadi, A., 2019, Green synthesis of silver-chitosan nanocomposite and their application as antibacterial material, *J. Phys.: Conf. Ser.*, 1153, 012135.
- [19] Susilowati, E., Ariani, S.R.D., Mahardiani, L., and Izzati, L., 2021, Synthesis and characterization chitosan film with silver nanoparticles addition as a multiresistant antibacterial material, *JKPK*, 6 (3), 371–383.
- [20] Jahangirian, H., Haron, M.J., Ismail, M.H.S., Rafiee-Moghaddam, R., Afsah-Hejri, L., Abdollahi, Y., and Vafaei, N., 2013, Well diffusion method for evaluation of antibacterial activity, *Dig. J. Nanomater. Biostruct.*, 8 (3), 1263–1270.
- [21] Pestov, A., Nazirov, A., Modin, E., Mironenko, A., and Bratskaya, S., 2015, Mechanism of Au(III) reduction by chitosan: Comprehensive study with ^{13}C and ^1H NMR analysis of chitosan degradation products, *Carbohydr. Polym.*, 117, 70–77.
- [22] Patra, J.K., and Baek, K.H., 2014, Green nanobiotechnology: Factors affecting synthesis and characterization techniques, *J. Nanomater.*, 2014, 417305.
- [23] Kalaivani, R., Maruthupandy, M., Muneeswaran, T., Hameedha Beevi, A., Anand, M., Ramakritinan, C.M., and Kumaraguru, A.K., 2018, Synthesis of chitosan mediated silver nanoparticles (AgNPs) for potential antimicrobial applications, *Front. Lab. Med.*, 2 (1), 30–35.
- [24] Maguire, C.M., Rösslein, M., Wick, P., and Prina-Mello, A., 2018, Characterisation of particles in solution – A perspective on light scattering and comparative technologies, *Sci. Technol. Adv. Mater.*, 19 (1), 732–745.
- [25] Danaei, M., Dehghankhold, M., Ataei, S., Davarani, F.H., Javanmard, R., Dokhani, A., Khorasani, S., and Mozafari, M.R., 2018, Impact of particle size and polydispersity index on the clinical applications of lipidic nanocarrier systems, *Pharmaceutics*, 10 (2), 57.
- [26] Regiel, A., Irusta, S., Kyzioł, A., Arruebo, M., and Santamaria, J., 2013, Preparation and characterization of chitosan-silver nanocomposite films and their antibacterial activity against *Staphylococcus aureus*, *Nanotechnology*, 24, 015101.
- [27] Marambio-Jones, C., and Hoek, E.M.V., 2010, A review of the antibacterial effects of silver nanomaterials and potential implications for human health and the environment, *J. Nanopart. Res.*, 12 (5), 1531–1551.